

Synthesis and characterization of organo-soluble aniline oligomer-based electroactive doped with gold nanoparticles, and application to electrochemical sensing of ascorbic acid



Wei-Fu Ji^a, Chieh-Ming Chu^a, Sheng-Chieh Hsu^a, Yi-De Lu^a, Yun-Chieh Yu^a, Karen S. Santiago^{b, **}, Jui-Ming Yeh^{a, *}

^a Department of Chemistry and Center for Nanotechnology, Chung-Yuan Christian University, Chung Li, 32023, Taiwan, ROC

^b Department of Chemistry, Research Center for the Natural and Applied Sciences, University of Santo Tomas, Espana, Manila, 1015 Philippines

ARTICLE INFO

Article history:

Received 5 June 2017

Received in revised form

29 August 2017

Accepted 15 September 2017

Available online 17 September 2017

Keywords:

Organo-soluble

Electroactive polyimide

Ascorbic acid sensor

ABSTRACT

Organo-soluble aniline oligomer-based electroactive polyimide (EPI) doped with gold nanoparticles (GNPs) applied in sensing ascorbic acid (AA) was presented. Conjugated aniline trimer (AT3) and aniline tetramer (AT4) were synthesized and characterized via ¹H NMR, FTIR, and MS spectroscopic studies. Subsequently, the organo-soluble electroactive polyimide (EPI) was prepared by chemical imidization of electroactive poly(amic acid) (EPAA), followed by characterization through FTIR and GPC analyses. Moreover, formation of reduced gold nanoparticles (GNPs) upon the surface of EPI was confirmed by XRD, SEM-EDS, TEM and ICP-OES. Based on CV studies, the redox capability of as-prepared materials was found to show a decreasing trend of EPI-4G > EPI-4 > EPI-3. The as-prepared EPI-4G modified carbon paste electrode (CPE) turned out best in sensing AA at lower oxidative potential with good sensitivity, relative low detection limit, broad linear dynamic range and best selectivity for a tertiary mixture of ascorbic acid (AA)/dopamine (DA)/uric acid (UA) compared to the other tested electrodes.

© 2017 Elsevier Ltd. All rights reserved.

1. Introduction

Ascorbic acid (AA), commonly known as vitamin C, is a required nutrient due to its anti-oxidant properties, thus often exists in large amounts in many foods and drinks. AA is also important in many human metabolic processes because of its redox property. This vitamin plays an essential role in biological, and is usually used to treat and prevent common colds and complex diseases [1] such as infertility, cancer, AIDS and mental illness. Thus, designing a facile and fast method to detect AA with a high selectivity and sensitivity is significant for application in food, cosmetics, pharmaceutical, and medical fields. Many techniques have been used in sensing AA, such as spectroscopic [2], chromatographic [3], enzymatic [4] and electroanalytical [5] methods. Among them, electrochemical methods are the best potential approaches because of their simplicity and high sensitivity toward AA. Therefore, the requirement for

materials having higher redox property is essential to fulfill the improvement in electrochemical sensor applications.

In recent years, there are many encouraging developments towards commercialization of electroactive polymers applied in electroluminescent devices, corrosion resistant coatings, electrostatic dissipation coatings, and electrochemical sensors [6–14]. However, one major problem associated with the large-scale commercial application is the limited processability of electroactive polymers. For example, polyaniline solution in N-methyl-2-pyrrolidinone (NMP) often leads to the formation of gels. Also, unsubstituted polythiophene and polypyrrole are not soluble in common organic solvents.

To overcome these problems, many researchers focused on the synthesis of electroactive oligomers of well-defined structures in the past decades. For example, Wei et al. reported the synthesis and characterization of amine-terminated aniline trimer (ACAT) [15]. Zhang et al. explored the synthesis of aniline tetramer and pentamer and study their redox properties [16]. Also, the polymeric derivatives for the aniline oligomers of well-defined structures have also evoked great research interests in academic studies and industrial applications. For example, Yeh et al. reported the

* Corresponding author.

** Corresponding author.

E-mail addresses: kssantiago@yahoo.com (K.S. Santiago), juming@cycu.edu.tw (J.-M. Yeh).

preparation and diverse applications of ACAT-based electroactive epoxy [17], polyimide [18], polyamide [19], polyurethane [20] and polyurea [21], etc. Among the aniline oligomer-derivative polymers, electroactive polyimide attracted extensive research interests due to the integration of high mechanical strength of polyimide and reversible redox/doping properties of conducting polymers. For example, Yeh et al. demonstrated that the mechanical strength of electroactive polyimide containing ACAT fragments was found significantly higher than that of conventional polyimide membrane [22]. However, published research reports in terms of aniline oligomer-based electroactive polyimide was usually prepared from thermal imidization. Research works related to organo-soluble aniline oligomer-based electroactive polyimide have seldom been mentioned.

On the other hand, several nanoparticles, including metals, oxides, and semi-conducting nanoparticles have been used to develop electrochemical sensor. For example, gold/silver nanoparticles, or silver-silica hybrid nanostructures used as sensor substrates have been explored by several laboratories [23–25]. Among these nanomaterials used as components in electrochemical sensors, gold nanoparticles (GNPs) have received intense interests because they exhibit several intriguing properties [26,27]. GNPs, with diameter of 1–100 nm, exhibit high surface energy and surface-to-volume ratio that offer a stable immobilization of huge amount of biomolecules maintaining their bioactivity. Moreover, GNPs permit fast and direct electron transfer between many electroactive species and electrode materials.

In this study, comparative studies of sensing AA with electroactive polyimide containing different chain length of conjugated diamines was presented. Moreover, the gold nanoparticle was reduced upon surface of electroactive polyimide to get the sensing of AA at lower oxidative potential with good sensitivity, relative low detection limit and broader linear dynamic range. First, the aniline trimer (AT3) and aniline tetramer (AT4) was synthesized by oxidative coupling reaction, followed by characterization by ^1H NMR, FTIR and Mass spectroscopy. Subsequently, organo-soluble EPI-4 and EPI-3 was prepared by reacting AT3 and AT4 with dianhydride to give electroactive poly(amic acid) (EPAA), followed by performing chemical imidization to convert EPAA into EPI. The as-prepared organo-soluble EPI was then characterized by ^1H NMR, FTIR and GPC. Moreover, the EPI-4 was immersed in 19 mL of 0.1 mM $\text{HAuCl}_4 \cdot 3\text{H}_2\text{O}$ aqueous solution for 6 h. The formation of reduced GNPs on the surface of EPI-4 was further confirmed by the XRD pattern, SEM-EDS, TEM and ICP-OES. Redox behavior of as-prepared electroactive materials can be observed by electrochemical CV studies and UV-visible absorption spectroscopy. The electrochemical sensor for sensitivity studies of AA sensing constructed by CPE modified with EPI-4G, EPI-4, EPI-3 and bare CPE was performed and compared. The selectivity studies of electrochemical sensor of CPE modified with EPI-4G, EPI-4, EPI-3, and bare CPE was also investigated by differential pulse voltammetric studies (DPV) towards a tertiary mixture of AA/UA/DA.

2. Experimental section

2.1. Chemicals and instrumentations

Aniline (Sigma-Aldrich, 99.5%) was distilled prior to use. 4,4'-diamino-diphenylamine sulfate hydrate (TCI, 97%), *N*-phenyl-1,4-phenylene diamine (Sigma-Aldrich, 98%), 4,4'-(4,4'-isopropylidene-diphenoxy)bis(phthalic anhydride) (Sechem, >99%), hydrazine (Alfa Aesar, 98%), and ammonium persulfate (APS, Sigma, 98%) were used as received without further purification. Acetic anhydride (J. T. Baker, > 99%), pyridine (J. T. Baker, > 99%), dimethyl formamide (DMF, J. T. Baker, 99%), *N,N*-dimethylacetamide (DMAC,

Macron, 99%), *N*-methyl-2-pyrrolidone (NMP, Macron, 99%), dimethyl sulfoxide (DMSO, Macron, 99%), tetrahydrofuran (THF, Macron, 99%), chloroform (CHCl_3 , Macron, 99%), L-ascorbic acid (AA, Sigma-Aldrich, 99%) were used as received without further purification. Hydrogen tetrachloroaurate(III) trihydrate ($\text{HAuCl}_4 \cdot 3\text{H}_2\text{O}$; Alfa Aesar, 99.99%), hydrochloric acid (HCl; Riedel-deHaën, 37%), ammonium solution (NH_4OH , Riedel-dehaën, 25%), and methanol (MeOH, Riedel-dehaën, 99.8%) were used as received. All reagents were reagent grade unless otherwise stated.

^1H NMR investigations were run on a Bruker 300 spectrometer, referenced to internal standard of tetramethylsilane (TMS). DMSO was used as solvent. Fourier-transformation infrared (FTIR) spectroscopic analysis was performed using an FTIR spectrometer (JASCO FT/IR-4100) at room temperature. Mass spectra were obtained using a Bruker Daltonics IT mass spectrometer model Esquire 2000 (Leipzig, German) with an Agilent ESI source (model G1607 – 6001). Weight-average and number-average molecular weights of EPI-3 and EPI-4 were determined on a Waters GPC-150CV (USA) equipped with a differential refractometer detector and a Styragel HT column using NMP as eluent and monodisperse polystyrenes as calibration standards.

Microstructures of EPI-4G membranes were imaged with a JEOL-200FX TEM (Japan). Samples for TEM study were cut into thin film with 60–90 nm thickness by a diamond knife. Electrochemical experiments were performed on a VoltaLab 50 (PST050) analytical voltammeter using a conventional three-electrode system. Electrochemical experiments were performed in a cell containing 20.0 mL phosphate buffer solution (PBS, 0.1 M, PH = 7) at room temperature, using a coiled platinum wire as the auxiliary electrode, a glass cell consisting of Ag/AgCl (3 M NaCl) as the reference electrode, and EPI- (EPI-3, EPI-4 and EPI-4G) modified carbon-paste electrode (CPE) as the working electrode.

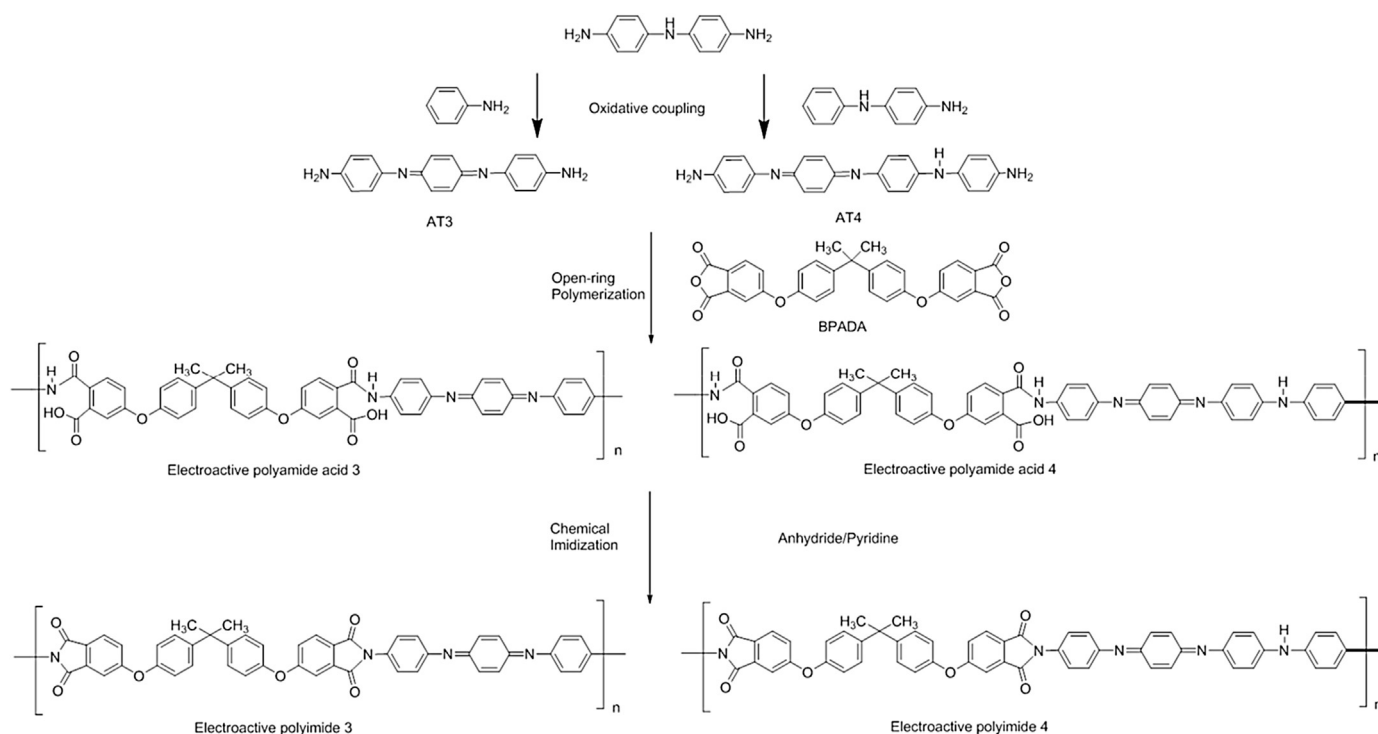
2.2. Synthesis of aniline oligomers

2.2.1. Synthesis of aniline trimer (AT3)

To synthesize AT3, aniline (1.48 g, 0.016 mol) and 4,4'-diaminodiphenylamine sulfate (4.73 g, 0.016 mol) were dissolved in HCl aqueous solution (1.0 N, 150 mL) containing 15 g of NaCl. A solution of ammonium persulfate (3.6 g, 0.016 mol) in HCl aqueous solution (1.0 N, 25 mL) was added at a rate of approximately 60 drops min^{-1} to the previously described solution maintained at operational temperature of 5 °C using a dropping funnel. The reaction mixture was stirred for 1 h at 5 °C. The resulting precipitate was collected through filtration, followed by washing with large amounts of HCl aqueous solution (1.0 N, 400 mL). Then, the filtrate was washed with NH_4OH solution (1.0 N, 100 mL) and followed by washing with copious amount of distilled water. Thus, a blue powder was further dried in dynamic vacuum oven at an operational temperature of 50 °C for 24 h. The crude product of AT3 was obtained as blue powder with a yield of ~40% [28].

2.2.2. Synthesis of aniline tetramer (AT4)

To prepare AT4, diphenylamine 1.84 g (0.01 mol) and 4,4'-diaminodiphenylamine sulfate (2.1 g, 0.01 mol) were dissolved in a ternary solvent system (100 mL of DMF, 20 mL of distilled water and 15 mL of HCl 1.0 N, 135 mL). A solution of ammonium persulfate (2.28 g, 0.01 mol) in HCl aqueous solution (1.0 N, 25 mL) was added at a rate of approximately 60 drops min^{-1} to the previously described solution at 0 °C using a dropping funnel. The reaction mixture was stirred for 1 h at 0 °C. It was then transferred into a 1000 mL of beaker containing 700 mL of distilled water to precipitate the product. The precipitate was collected by vacuum filtration through a Buchner funnel and washed by 400 mL of 1.0 N HCl, followed by washing with 100 mL of 1.2 N ammonium hydroxide



Scheme 1. Preparation of oligo-aniline and organo-soluble electroactive polyimide by using oxidative coupling and chemical imidization, respectively.

solution and excess amount of distilled water. After drying at 50 °C under dynamic vacuum oven for 24 h, the crude product of AT4 was obtained as blue powder at a yield of ~35% [29].

2.3. Synthesis of EPI-3 and EPI-4

BPADA (0.52 g, 1 mmol) was added to 8.0 g of DMAc at room temperature with continuous stirring for 30 min. A solution containing AT3/AT4 (0.289 g/0.379 g, 1 mmol) in another 8.0 g of DMAc were prepared under magnetic stirring, respectively. Dianhydride of BPADA was reacted with AT3/AT4, followed by stirring for 24 h to generate electroactive poly(amic acid) (EPAA-3 and EPAA-4). In order to give organo-soluble electroactive polyimide (EPI-3 and EPI-4), the previous solution containing electroactive poly(amic acid) was further processed by chemical imidization reaction by adding the mixture of acetic anhydride/pyridine (0.102/0.079, v/v, 0.181 mL) to the previous solution containing EPAA-3 or EPAA-4 under stirring for 1 h. Subsequently, the mixtures were further stirred at operational temperature of 150 °C for 3 h to gain homogeneous polyimide solutions. The as-prepared EPI solutions were slowly added dropwise to an excess amount of methanol to precipitate the product, followed by collecting by filtration and subsequently washed by hot methanol. After dynamic drying at operational temperature of 60 °C in vacuum overnight, the as-prepared EPI-3 and EPI-4 in the form of blue powder were collected at the yield of ca. ~80% for both final blue products. The flowchart for the preparation of EPI-4 and EPI-3 was shown in Scheme 1.

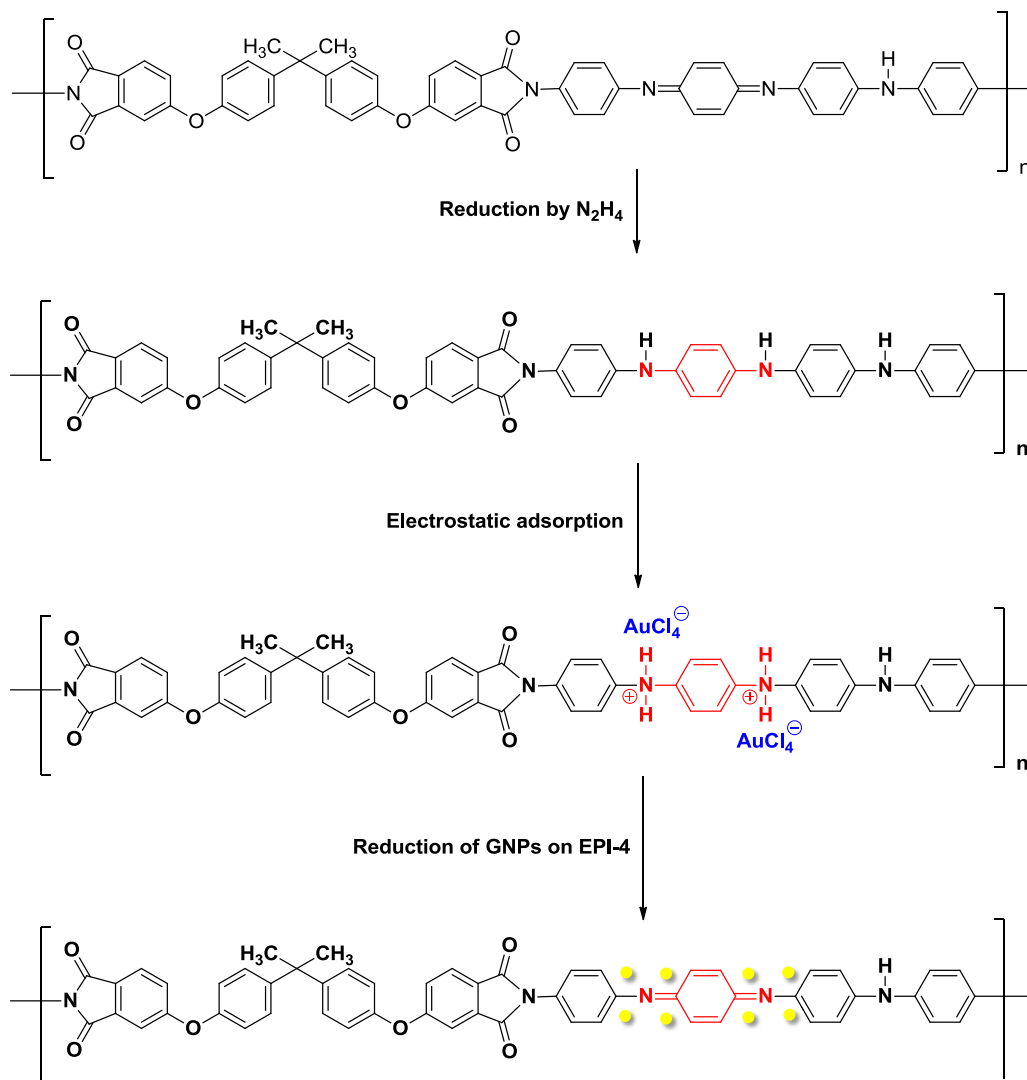
2.4. Preparation of EPI-4G

For the preparation of EPI doped with GNPs, EPI-4 was chosen instead of EPI-3 because of higher redox capability of EPI-4 as compared to that of EPI-3. As a representative procedure to prepare

the EPI-4G: first, 0.1 g of well-prepared EPI-4 fine powder was dispersed into 10 mL of 1.0 M NH_4OH containing 1 mL of hydrazine solution, followed by stirring for 24 h. The mixture was filtered, washed by distilled water until pH = ~7, followed by freeze-drying treatment at operational temperature of -42 °C for 24 h. Moreover, the 0.1 g of as-prepared reduced form of EPI-4 blue powder was immersed in 19 mL of 0.10 mM $\text{HAuCl}_4 \cdot 3\text{H}_2\text{O}$ aqueous solution at room temperature for 6 h. The EPI-4G powder was subsequently collected by centrifugal filtration, and followed by washing with excess amount of distilled H_2O . After drying at 50 °C in vacuum oven for 24 h, the as-prepared EPI-4G was collected as blue fine powder. The flowchart for the preparation of EPI-4G was shown in Scheme 2.

2.5. Redox property of as-prepared materials confirmed by electrochemical cyclic voltammetry studies

In this study, the redox property of different electroactive coating materials (e.g., EPI-3, EPI-4 and EPI-4G) was determined by casting the materials onto an indium tin oxide (ITO) electrode (working electrode), followed by performing a series of electrochemical cyclic voltammetry (CV) studies. First, 0.05 g of as-prepared EPI-4G, EPI-4, and EPI-3 were dissolved separately in 5 mL of DMAc under magnetic stirring for 6 h. Moreover, the ITO electrode ($5 \times 5 \text{ cm}^2$) coated with different electroactive materials was obtained through spin-coating (spinning rate of 3000 rpm) the as-prepared DMAc coating solutions, followed by heating at programmed temperature of 120 °C for 1 h. Cyclic voltammetry (CV) was conducted on a VoltaLab 50 (potentiostat/galvanostat) electrochemical workstation in 40 mL of 1.0 M H_2SO_4 aqueous solution. A platinum foil served as auxiliary electrode, and Ag/AgCl (3 M NaCl solution) electrode was used as reference electrode. All electrochemical CV measurements were performed in a double-wall jacketed cell at constant operational temperature of 25 °C.



Scheme 2. Possible mechanism for the formation of EPI-4G.

2.6. Electrochemical sensing of AA

The flowchart for the preparation of electrochemical sensor constructed by carbon paste electrode (CPE) modified with different electroactive polymer samples for AA detection was shown in Fig. 1. First, 0.04 g of samples (*i.e.*, EPI-3, EPI-4G, EPI-4 and

EPI-3) was mixed with 0.05 g of graphite powder and 0.01 g of paraffin oil, followed by grinding with mortar and pestle. Subsequently, the as-prepared paste was firmly packed into the cavity of Teflon tube, which is 3 mm in diameter and served as working electrode. An electrical contact was established via copper rod through the center of tube. Suitable packing can be obtained to

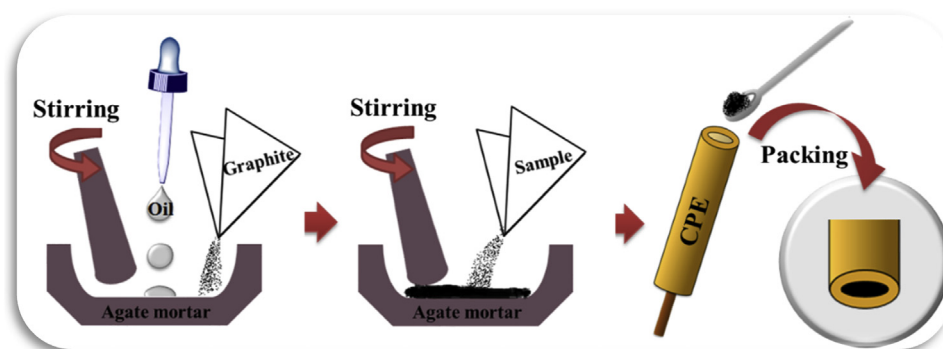


Fig. 1. The flowchart for preparing of CPE modified with different samples (*i.e.*, EPI-3, EPI-4 and EPI-4G).

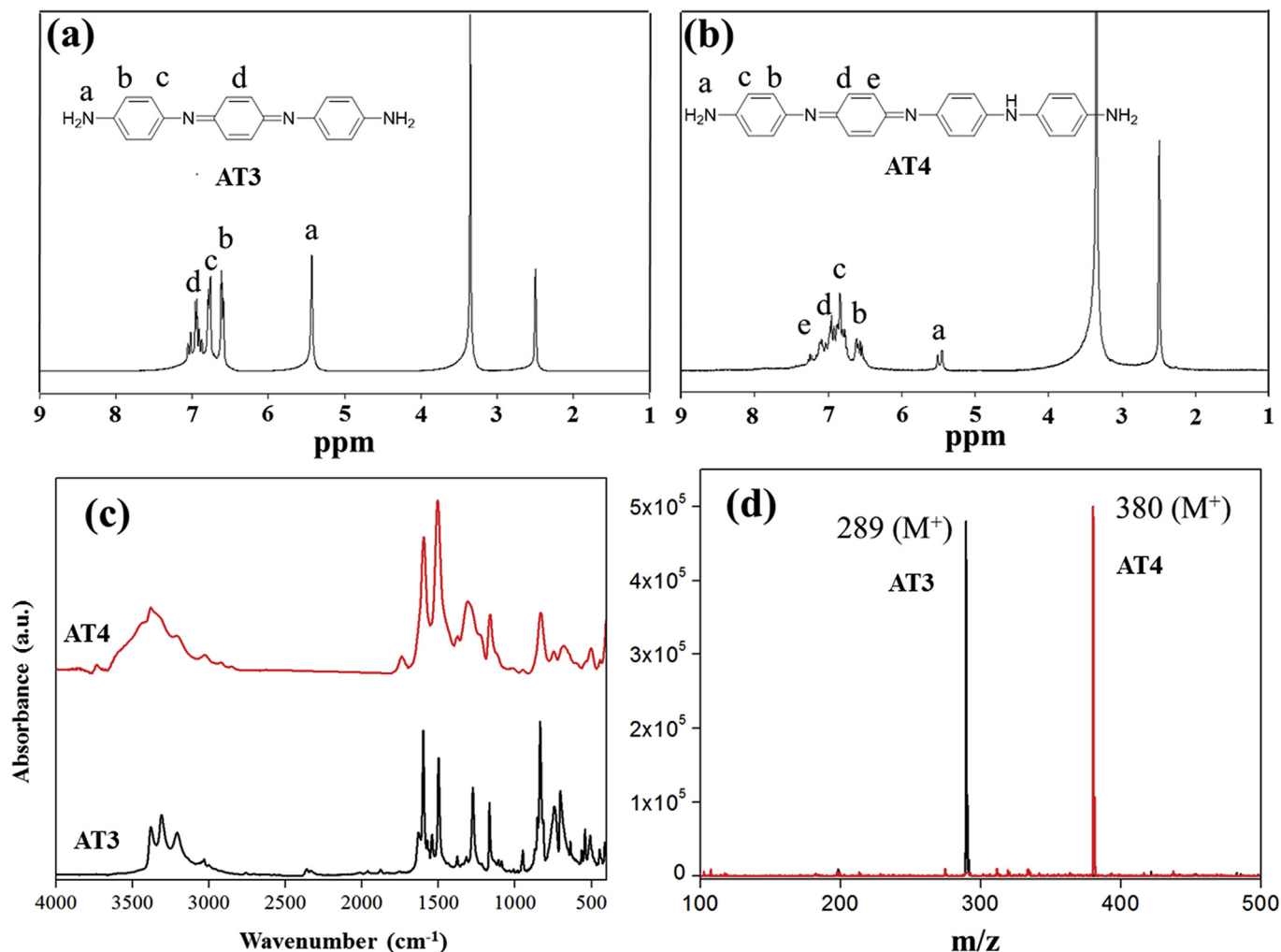


Fig. 2. Characterization of AT3 and AT4 as determined by (a)&(b) ¹H NMR, (c) FTIR and (d) Mass spectroscopy.

compact electrode surface toward bond paper until surface was smooth. Voltammetric measurements were performed by using VoltaLab 50 and AutoLab electrochemical workstation in 20 mL of 0.1 M phosphate buffer solution (PBS). The electrochemical sensing of as-prepared materials was established by using a three-electrode system equipped in a double-wall jacketed cell. Ag/AgCl (3 M NaCl solution) electrode was used as reference electrode and platinum foil was served for the counter electrode, respectively. The as-prepared CPE electrodes modified with EPI-3, EPI-4 or EPI-4G employed as working electrode for sensing ascorbic acid were prepared. All electrochemical sensing measurements were investigated at constant operational temperature of 25 °C.

2.7. Monitoring the redox structure of AT4 existed in EPI-4/EPI-4G by UV-visible absorption spectroscopy

In this study, UV-visible absorption spectroscopy was used to monitor the change of redox structure of AT4 existing in EPI-4/EPI-4G. Initially, the as-prepared EPI was first reduced, and the AT4 of EPI-4 towards fully reduced form of AT4 by adding 0.1 g of as-prepared of EPI-4 into 13 mL of N₂H₄ solution (3 mL of N₂H₄/10 mL of NH₄OH). Mixed product was then treated by freeze-drying for 24 h to get rid of liquid component, denoted as *sample 1*. Subsequently, the as-obtained 0.1 g of freeze-dried fine powder was then dispersed in 19 mL of 0.1 mM HAuCl₄·3H₂O aqueous solution

for 6 h under magnetic stirring by oxidizing the fully reduced form of AT4 in EPI-4 and reducing the AuCl₄⁻ to GNPs simultaneously, leading to the formation of EPI-4G. The as-obtained EPI-4G was subsequently treated by freeze drying for another 24 h, denoted as *sample 2*. Moreover, the ~0.1 g of freeze-dried EPI-4G was then dispersed in 10 mL of 10 mM AA solution under magnetic stirring for 3 h, followed by freeze-drying treatment for 24 h, denoted as *sample 3*. All three freeze-dried samples were dissolved in 3 mL of DMAc for the following studies of UV visible absorption spectroscopy.

3. Results and discussion

3.1. Characterization of AT3 and AT4

The representative ¹H NMR, FTIR and LC-Mass spectra of AT3 and AT4 were shown in Fig. 2. From Fig. 2 (a), the ¹H NMR spectra found at the position of δ = 5.45 ppm and δ = 7.25 to 6.50 ppm could be assigned to be primary amine protons (-NH₂) and splitting of aromatic proton of AT3, respectively. Moreover, the signals of AT4 appearing at the position of δ = 5.5 ppm shown in Fig. 2 (b) could be also assigned to the primary amine protons (-NH₂), and the relative intensity of signals found at the position of δ = 7.9 to 6.8 ppm represents the expected splitting of aromatic proton signals of AT4. Furthermore, the FTIR spectra of AT3 and AT4 were shown in Fig. 2

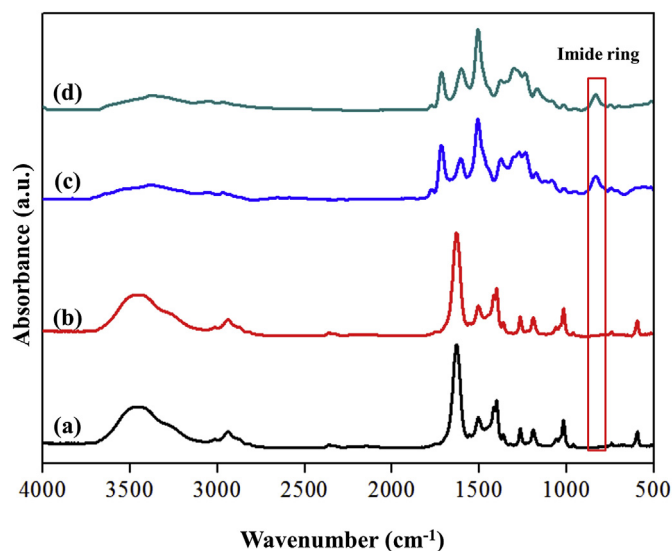


Fig. 3. The representative FTIR spectra for (a) EPAA-3, (b) EPAA-4, (c) EPI-3 and (d) EPI-4.

(c). The characteristic absorption bands of FTIR spectra found at position of 3309 and 3385 cm^{-1} may be attributed to the terminal -NH_2 of AT3 and AT4. Moreover, the characteristic absorption bands of FTIR spectra appearing at the position of 1597, 1496 cm^{-1} and 1599, 1505 cm^{-1} could be assigned to the vibrational bands of quinoid (Q) rings and benzenoid (B) rings of AT3 and AT4, respectively. Finally, the molecular ion peaks appeared at the position of 289 and 380 can be assigned to be the molecular weight of AT3 and AT4, respectively, as shown in Fig. 2 (d). These experimental data were found to be consistent with theoretical molecular weight of AT3 and AT4, respectively [30,31].

3.2. Characterization and solubility of organo-soluble EPAA and EPI

The as-prepared electroactive diamine of AT3 and AT4, synthesized in section 3.1, was further reacted with dianhydride of BPADA to give an organo-soluble electroactive poly(amic acid) (EPAA), followed by performing chemical imidization reactions of EPAA with suitable amount of acetic anhydride/pyridine to give series of organo-soluble electroactive polyimides (EPI). The chemical imidization reaction of converting EPAA into EPI was observed by monitoring FTIR spectra, as shown in Fig. 3. The characteristic peaks of as-prepared EPAA (EPAA-3/EPAA-4) were verified at a wavenumber range of 3400–3600 cm^{-1} , as shown in Fig. 3 (a) and Fig. 3 (b), corresponding to the hydroxyl group that from carboxylic acid of EPAA. In addition, the characteristic absorption peaks found at the position of 1596 and 1503 cm^{-1} were assigned to the stretching modes of $\text{N}=\text{Q}=\text{N}$ and $\text{N}-\text{B}-\text{N}$, respectively, where Q and B corresponded to the quinoid ring and benzene ring. After reacting with acetic anhydride/pyridine, the EPAA were converted

into EPI by performing the chemical imidization. It could be noted that the imide ring of EPI and carboxylic acid of EPAA appeared and disappeared simultaneously. As shown in Fig. 3 (c) and (d), the FTIR spectra of EPI (EPI-3 and EPI-4) were found to reveal a characteristic absorption band at a wavenumber of 742 cm^{-1} , which corresponded to the deformation of imide group. Moreover, the characteristic absorption band of EPAA found at the position of 3400–3600 cm^{-1} was found to disappear [32]. It indicated that the complete conversion of EPAA into EPI by performing the chemical imidization process.

Moreover, the solubility of as-prepared organo-soluble EPI-3 and EPI-4 in common organic solvents were also studied and summarized in Table 1. It should be noted that the as-prepared EPI exhibited quite good solubility in NMP, DMAc, DMF and DMSO at room temperature. However, the as-prepared EPI was found to reveal partial solubility in THF and chloroform at room temperature. Number-average molecular weight (\overline{M}_w), weight-average molecular weight (\overline{M}_n) and polydispersity index (PDI) of EPI-3 and EPI-4 was also shown in Table 1. For example, \overline{M}_w , \overline{M}_n and PDI of EPI-3 were 96,000, 21,000 and 4.6, respectively. Moreover, \overline{M}_w , \overline{M}_n and PDI of EPI-4 were 99,000, 20,000 and 4.8, respectively.

3.3. Characterization of GNP formation by XRD, SEM-EDS, TEM and ICP-OES

After the characterization of organo-soluble EPI, the EPI4-G was prepared by immersing the EPI-4 into 5 mL of 0.1 mM $\text{HAuCl}_4 \cdot 3\text{H}_2\text{O}$ for 6 h. The appearance of gold nanoparticles (GNPs) on EPI was identified by XRD and TEM. The representative XRD patterns of EPI-4 and EPI-4G were shown in Fig. 4 (a). It should be noted that, as compared to EPI-4, the diffraction pattern of EPI-4G was showed four additional peaks and observed at the position of $2\theta = 38.01^\circ$, 43.96° , 64.50° , and 77.42° , which may correspond to the Bragg reflections from (111), (200), (220) and (311) Au planes [33]. Moreover, the SEM-EDS spectra of EPI-4G was found to display obvious Au peak, as shown in Fig. 4 (b). Furthermore, the TEM image of EPI-4G was also investigated in magnification ($\times 200$ K), as shown in Fig. 4 (c). It should be noted that the black spots of EPI-4G, appeared in Fig. 4 (c), was GNP with the size of ~ 30 nm in diameter. Finally, the weight percentage of reduced GNPs formed onto the surface of EPI-4 was determined by ICP-OES. It had showed that the Au reduced on the EPI-4 was 905 ppm.

The mechanism was described that AuCl_4^- ions are selectively adsorbed by the protonated imine sites on the surface of EPI-4 with the aid of electrostatic effects, promoting further formation of the complexes. These complexes serve as the specific active sites for the formation of Au^0 nuclei because of electron transfer from the imine sites to AuCl_4^- , facilitating the simultaneous oxidation of the trimer segment in the EPI-4G and reduction of AuCl_4^- . AuCl_4^- ions are further reduced on the surface of Au^0 nuclei by autocatalytic surface reduction, leading to the growth of Au^0 nuclei and the successful formation of a uniform and ultrafine AuNPs distribution.

Table 1
Solubility of Electroactive Polyimide ^a, Viscosity Test ^b and GPC test ^c.

Sample code	Solvent						η (cPs.)	$\frac{\overline{M}_w}{\overline{M}_n}$ $\times 10^4$	PDI
	NMP	DMAc	DMF	DMSO	THF	CHCl_3			
EPI-3	++	++	++	++	±	±	3.9	9.6 2.1	4.6
EPI-4	++	++	++	++	±	±	4.1	9.9 2.0	4.8

^a Qualitative solubility was measured with 1 mg of a sample in 1 mL of organic solvent. ++ = Soluble at room temperature; ± = Partially soluble at room temperature.

^b Measured at polymer concentration of 0.5 g/dL in NMP at room temperature.

^c Relative to PS standards, using NMP as the eluent.

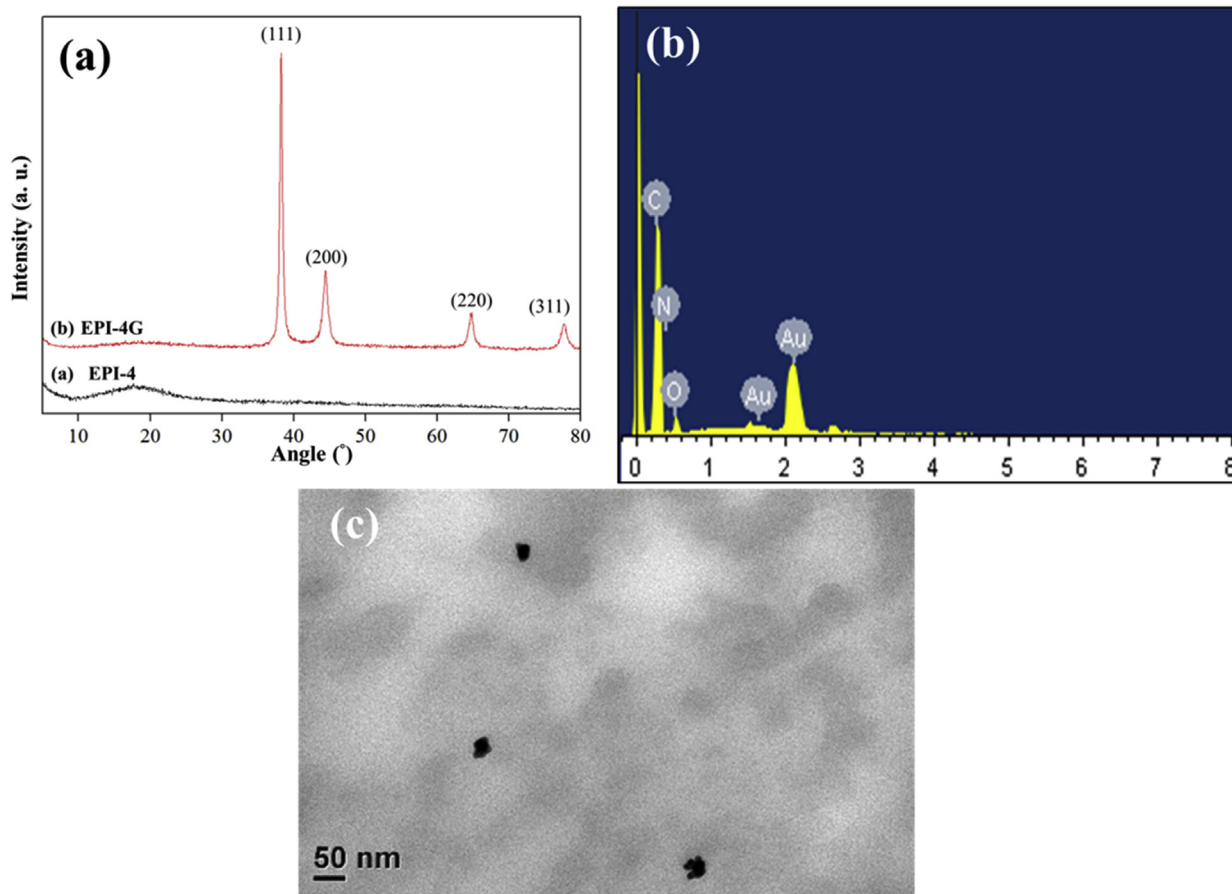


Fig. 4. Characterization of EPI-4G as determined by (a) XRD, (b) SEM-EDS spectroscopy and (c) TEM at magnification of x 200 k.

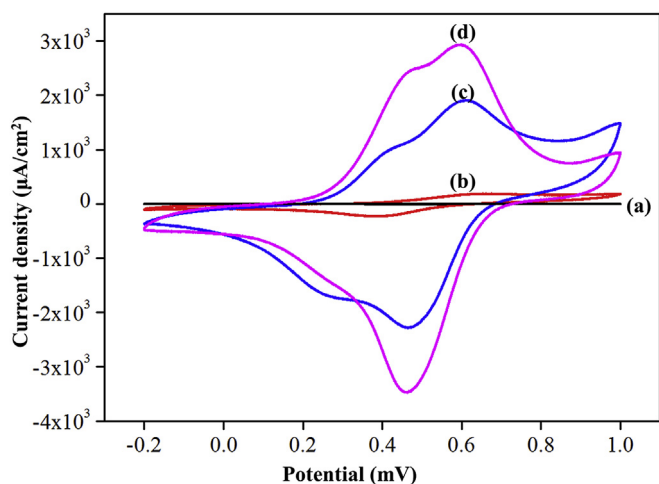


Fig. 5. Electrochemical cyclic voltammetry for (a) ITO, (b) EPI-3, (c) EPI-4 and (d) EPI-4G as measured in 1.0 M H₂SO₄ aqueous solution with scan rate of 50 mV/s.

3.4. Redox capability of materials measured by electrochemical CV studies

To investigate the redox capability, all as-prepared electroactive materials were examined in a strongly acidic electrolyte composed of aqueous 1.0 M H₂SO₄ solution by performing a series of electrochemical cyclic voltammetry (CV) studies. Fig. 5 exhibited the redox capability of bare ITO, EPI-3, EPI-4, and EPI-4G. As a control

experiment, the CV curve of bare ITO electrode was studied and no redox peak was found. EPI-3 was found to show relatively small peak of redox current = $\sim 100 \mu\text{A cm}^{-2}$, as shown in Fig. 5 (b). Moreover, the EPI-4 was found to reveal maximum redox current = $\sim 2000 \mu\text{A cm}^{-2}$. It indicated that EPI-4, with longer conjugated structure of diamine, exhibited higher redox capability than that of EPI-3 based on the electrochemical CV studies. After doping with small amount of GNPs, the maximum redox current of EPI-4G was found to increase up to $\sim 3000 \mu\text{A cm}^{-2}$. It implied that the EPI-4 doped with conductive GNPs do effectively enhance the redox capability of EPI-4 as shown in Fig. 5 (c) and (d). To sum up, the redox capability of as-prepared electroactive materials showed a decreasing trend: EPI-4G > EPI-4 > EPI-3.

3.5. Kinetic parameters study of CPE modified with EPI-4G

The effect of scan rate on the performance of CPE modified with EPI-4G in 0.1 M PBS (pH = 7) towards oxidation of 400 μM AA was also studied for kinetic parameters. The results of varying the scan rates from 10 to 300 mV s^{-1} are shown in Fig. 6(A). The oxidation current of AA increased as the scan rate rises from 10 to 500 mV s^{-1} . Additionally, the linear relationship was plotted between peak current (I_p) and square roots of scan rates ($\nu_{1/2}$), the observed linear regression equation is; $I_p (\mu\text{A}) = 0.165 \nu_{1/2}(\text{Vs}^{-1})^{1/2} + 8.3623$, $R^2 = 0.9984$.

Meaning that the electrode reaction of AA oxidation is controlled by diffusion based electron transfer reaction, as presented in Fig. 6(B). Moreover, the plots of peak potential (E_p) versus $\log \nu$ (Fig. 6 (C)), the linear equation of this straight line is obtained

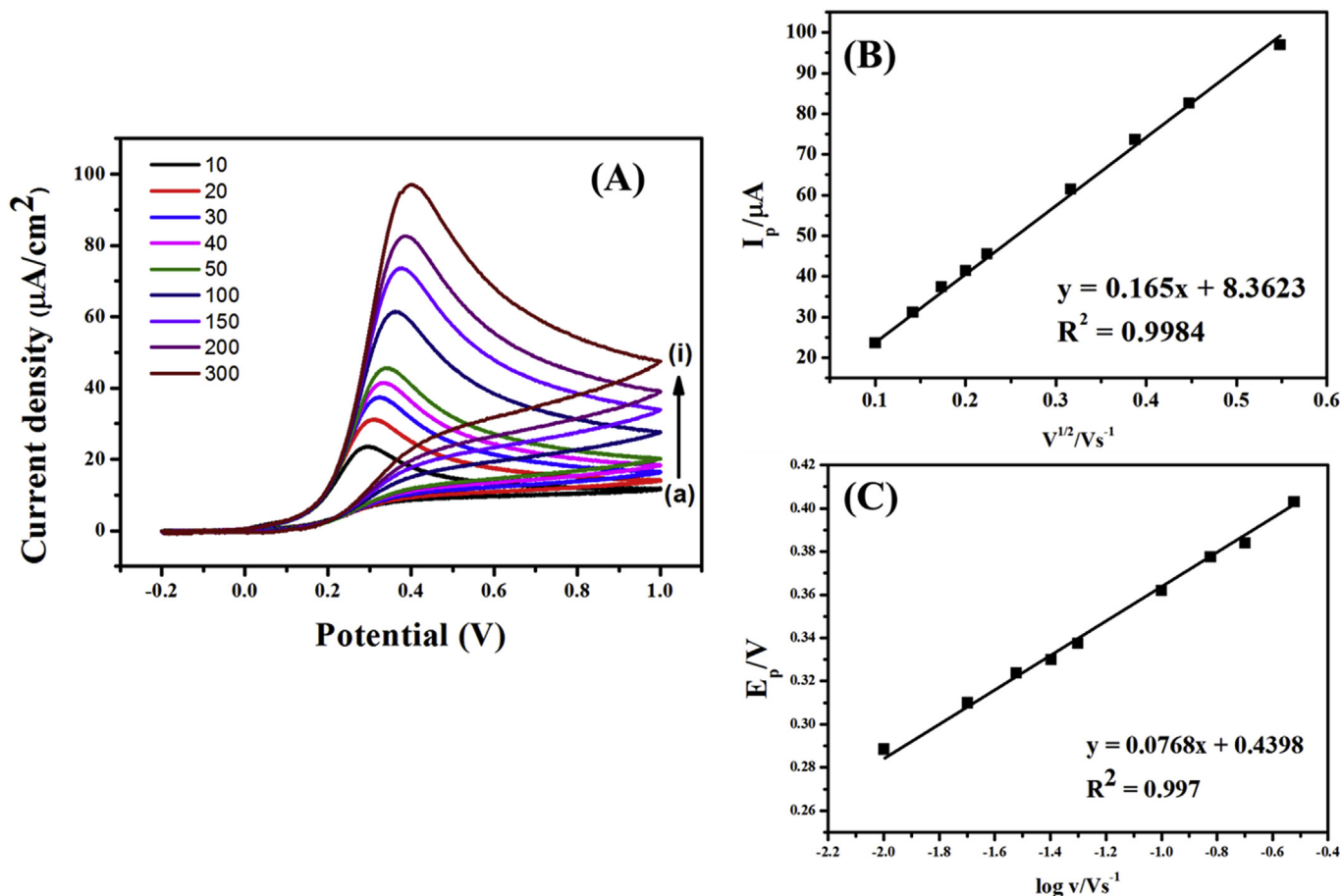


Fig. 6. (A) Cyclic voltammograms obtained of EPI-4G in PBS (pH ~ 7) at different scan rates (curves a to g: 10, 20, 30, 40, 50, 100, 150, 200, 300 mVs⁻¹) in the presence of 400 μM AA. (B) The plot between I_p vs. square roots of scan rates ($v^{1/2}$) (C) The plot of E_p vs. $\log v$.

as; $E_p = 0.0768 \log(v) + 0.4398$, $R^2 = 0.997$, was used to further investigate the mechanism of electrocatalysis of AA on the modified electrode, Using Eq. (1), for a fully irreversible diffusion-controlled system. The anodic peak potential can be evidenced by Ref. [34]:

$$E_p = \frac{2.303RT}{2(1-\alpha)n_aF} \log v + k$$

Where, α is the electron transfer coefficient, R ($R = 8.314 \text{ J K}^{-1} \text{ mol}^{-1}$) is the rate constant, F (96485 C mol^{-1}) is Faraday constant and T (298 K) is room temperature, and n_a is the number of electrons involved in the rate-determining step. Herein, the Tafel slope of 0.215 V/decade was calculated from Fig. 9(C), which indicates that single-electron transfer was involved in the rate-limiting step assuming a transfer coefficient of $\alpha = 0.61$.

3.6. Electrochemical sensing of AA

In this study, the electrocatalytic activity of as-prepared materials was used to detect AA by CV and amperometry. Fig. 7 showed the voltammograms corresponding to bare CPE, EPI-3, EPI-4 and EPI-4G modified electrodes in 0.1 M PBS (pH = 7) of 2 mM AA concentration with scan rate of 50 mV s⁻¹.

In the presence of 2 mM AA in PBS, a small oxidation current ($\sim 20 \mu\text{A cm}^{-2}$) of bare CPE occurred at a more positive potential of ~ 20 mV, as shown in Fig. 7 A (a). Moreover, it should be noted that the oxidant current of CPE modified with EPI-3, EPI-4 and EPI-4G was found to be ~ 80 , ~ 100 and $\sim 120 \mu\text{A cm}^{-2}$, respectively. It may

imply that the as-prepared materials showing the decreasing trend for sensitivity of AA detection: EPI-4G > EPI-4 > EPI-3.

Fig. 7 (B) showed the typical amperometric responses to AA by bare CPE and CPE modified with EPI-3, EPI-4, and EPI-4G at an applied potential of 390 mV in a 30 mL of PBS solution (pH = 7) under constant stirring. The current response increased gradually and accompanied with an increase in AA concentration. It should be noted that the CPE modified with EPI-4G resulted in a sudden increase in current response of AA. The sensitivity of CPE modified with EPI-4G was calculated to be $58.56 \mu\text{A mM}^{-1}$, which is 2.77-fold, 2.97-fold and 3.2-fold higher than those of CPE modified with EPI-4, EPI-3 and bare CPE, respectively, as shown in Table 2.

At low concentration, the bare CPE as well as CPE modified with EPI-3, EPI-4 and EPI-4G all displayed a direct linear relationship between the current response and AA concentration at a constant potential of 390 mV, as shown in Fig. 7 (C). However, the slope for CPE modified with EPI-4G was steep as compared to those of other electrodes (Scheme 3). On the gradual addition of different quantities of AA in a strongly stirred PBS solution equipped with CPE modified with EPI-4G, allowed detection of AA with high sensitivity ($58.56 \mu\text{A mM}^{-1}$) and a high correlation coefficient ($r = 0.992$).

In contrast, at higher AA concentrations (0.1–1 mM), the relationship between the responses and the concentration of AA can be described by a two-parameter sigmoidal equation [35].

$$j = j_{\max}[1 - \exp(-c/b)]$$

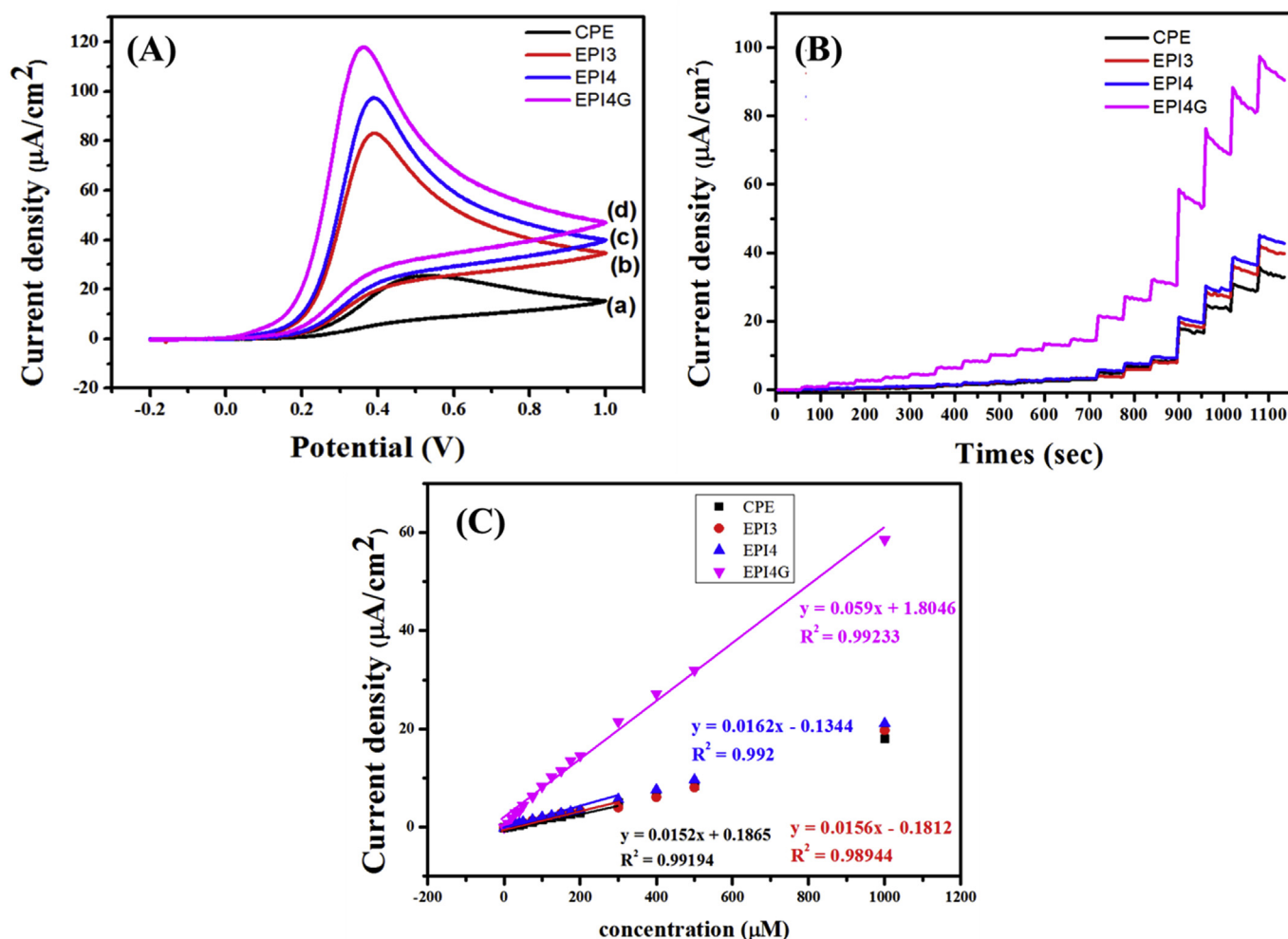


Fig. 7. (A) Cyclic voltammograms of (a) bare-CPE, (b) EPI-3, (c) EPI-4 and (d) EPI-4G modified electrodes in PBS (pH=7) with 2 mM AA concentrations with scan rate of 50 mV s⁻¹. (B) Typical Amperometric response obtained with (a) bare-CPE, (b) EPI-3, (c) EPI-4 and (d) EPI-4G modified electrode at 390 mV with successive additions of AA into 30 mL of PBS. (C) The corresponding calibration plot for current density vs. [AA] of (a) bare-CPE, (b) EPI-3, (c) EPI-4 and (d) EPI-4G modified electrodes.

where j represents the oxidation current, j_{\max} is the maximum value obtained at a sufficiently high concentration of AA, c is the concentration of AA, and b is an empirical coefficient characterizing the steepness of j , c transient, where $j_{\max} = 127.04 \mu\text{A cm}^{-2}$ and $b = 1.63 \text{ mM}$ with a correlation coefficient of $r = 0.9923$. However, such a fixed equation for j vs. c is inconvenient to use; therefore, the logarithm of the abscissa of calibration curve was used to generate a linear relationship. The slope of linear curve represents sensitivity of electrode. The defined sensitivity of CPE modified with EPI-4G, EPI-4, EPI-3, and bare CPE were 58.56, 21.13, 19.71, and 18 $\mu\text{A}/\text{mM}$, respectively. Moreover, oxidation current increased with the

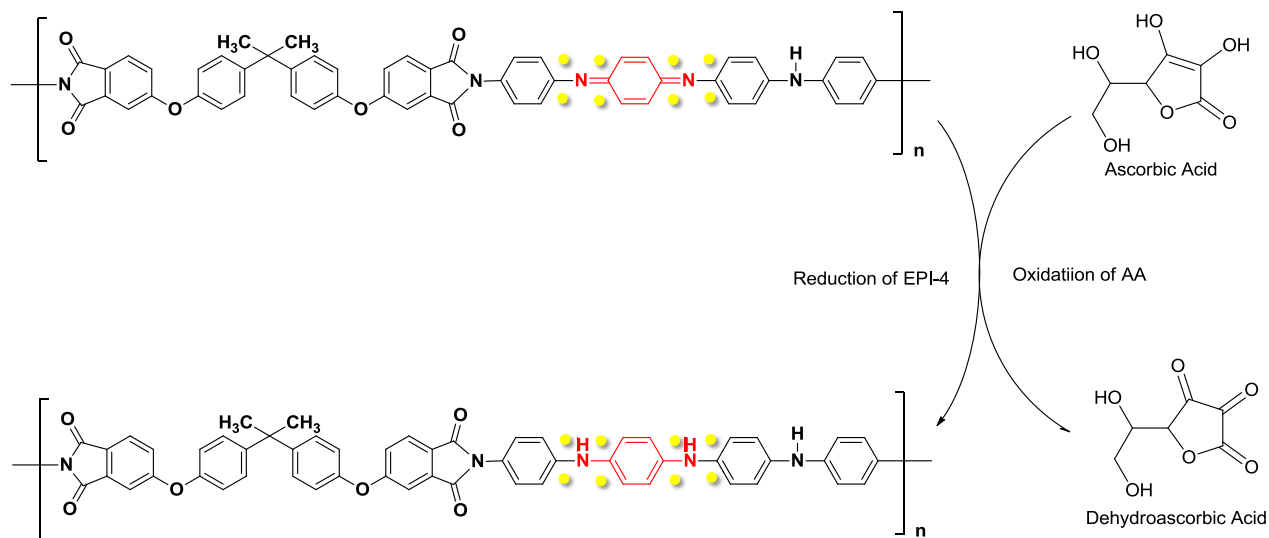
addition of AA and achieved a steady state after 2 s. This result indicated that CPE modified with EPI-4G is a rapid-response sensor with high sensitivity, wide LDR, and low LOD. A comparison of the sensitivity, LOD, and LDR for the other samples is given in Table 2. As seen in this comparison, the designed sensor exhibited high sensitivity, a relatively LOD, and a broad LDR.

3.7. Redox structure of AT4 existing in EPI-4/EPI-4G monitored by UV-visible absorption spectroscopy

It should be noted that all three samples exhibited two broad

Table 2
Comparison for the sensitivity, LOD and LDR of electrodes modified with different materials for AA detection.

Materials/Electrode type	Sensitivity($\mu\text{A} \cdot \text{mM}^{-1}$)	Limit of detection (LOD) (μM)	Linear dynamic range (LDR) (μM)	Ref.
EPA/CPE	24.2	7.1	50–450	[37]
AF-MWCNT-EPI/CPE	27.5	4.1	50–700	[38]
DPSA-doped nanoPANI/SPE	10.75	8.3	0.5–8 mM	[39]
Polyaniline(PANI)/SCPE	17.7	30 ± 3	30–270	[40]
AuNPs@polyaniline core–shell nanocomposites/GCE	–	8	20–1600	[41]
Au-PEDOT/ PANIS/Au/GCE	0.875	2.5	5–300	[42]
CPE	18	80.25	80–2000 μM	[43]
EPI3/CPE	19.71	34.48	10–200 μM	This work
EPI4/CPE	21.13	34.36	10–200 μM	This work
EPI4G/CPE	58.56	18.49	10–1000 μM	This work



Scheme 3. The redox mediation between AA and EPI-4G.

absorption bands with λ_{\max} at ca. 320 nm and 580–630 nm. The absorption band (band I) at ca. 320 nm is associated with the π - π^* transition of the conjugated ring system. The second band (band II) at ca. 600 nm has been assigned as a benzenoid to quinoid excitonic transition [36]. First, for the sample 1, UV-visible absorption spectrum of freeze-dried EPI-4 was found to exhibit higher absorption band at $\lambda_{\max} = 320$ nm and lower absorption band at 600 nm, as shown in the black line of Fig. 8 (a). Upon doped with GNPs, for the sample 2, the UV-visible absorption spectrum of freeze-dried EPI-4G was found to decrease in intensity of $\lambda_{\max} = 320$ nm and increase in intensity of $\lambda_{\max} \sim 600$ nm, simultaneously, as shown in the blue line of Fig. 8 (b). It indicated that as the reduced GNPs formed onto the surface of EPI-4, the fully reduced form of AT4 existed in EPI-4 was oxidized to emeraldine base (EB) form of AT4. Moreover, sample 3, the UV-visible absorption spectrum of freeze-dried EPI-4G after treating with AA was found to reveal increase in intensity of $\lambda_{\max} = 320$ nm and decrease in intensity of $\lambda_{\max} \sim 600$ nm, simultaneously, as shown in the red line of Fig. 8 (c). It implied that, in this study, the proposed electrochemical sensor constructed by CPE modified with EPI-4G for AA detection,

the EB form of AT4 existed in EPI-4G was reduced towards the fully reduced structure of AT4 as the AA was oxidized at the same time.

3.8. Differential pulse voltammetric responses for tertiary mixtures of AA, UA and DA

To study the selectivity of constructed electrochemical sensor, a tertiary mixture of 20 μ M ascorbic acid (AA)/dopamine (DA)/uric acid (UA) was employed. Differential pulse voltammograms (DPV) were recorded for a mixture of 20 μ M of DA, 20 μ M of AA and 20 μ M of UA for bare CPE, CPE modified with EPI-3, EPI-4 and EPI-4G in 0.1 M PBS (pH = 7), the experiments were carried out using DPV in the range of -0.3–0.8 V, as shown in Fig. 9. It should be noted that the selectivity of bare CPE (Fig. 9 (a)) is quite poor for tertiary mixture of AA/DA/UA. Moreover, the CPE modified with EPI-3 and EPI-4 showed improved selectivity for the tertiary mixture of AA/DA/UA, as shown in Fig. 9 (b) and (c). However, just two distinct voltammetric peaks can be found. In contrast, the CPE modified

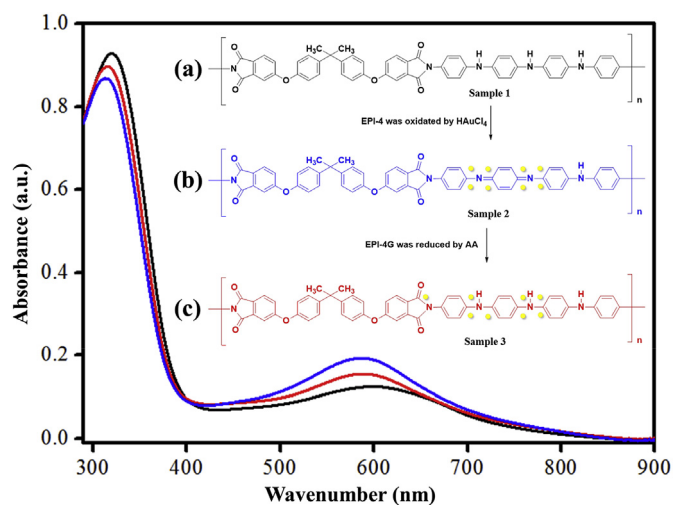


Fig. 8. The representative UV-visible absorption spectra for (a) EPI-4, (b) EPI-4G and (c) EPI-4G (after reacted with AA).

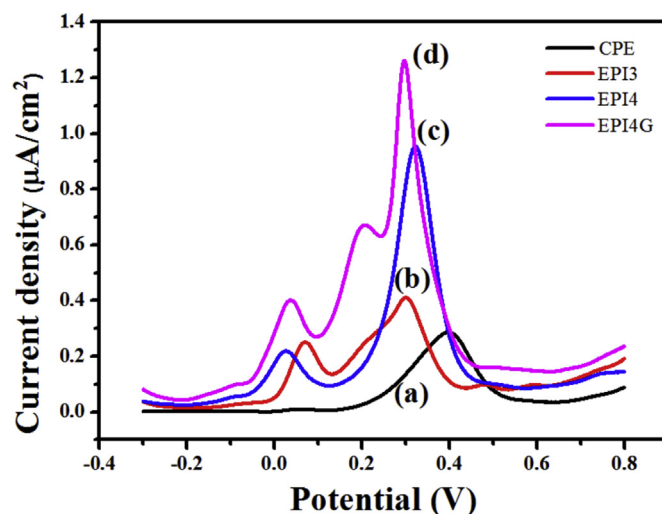


Fig. 9. Differential pulse voltammograms obtained with (a) bare-CPE, (b) EPI-3, (c) EPI-4 and (d) EPI-4G modified electrodes for a tertiary mixture of 20 μ M AA/DA/UA in 0.1 M PBS.

with EPI-4G was found to exhibit excellent selectivity and three distinct voltammetric peaks can be resolved at the potential of 40, 200, and 296 mV, which can be corresponded to the oxidation of AA, DA, and UA, respectively.

4. Conclusions

In this work, we present the first preparation of organo-soluble aniline oligomer-based electroactive polyimide (EPI) doped with gold nanoparticles (GNPs), which was later on applied in sensing of ascorbic acid (AA). The aniline trimer (AT3) and aniline tetramer (AT4) were synthesized by oxidative coupling reactions between 4,4'-diaminodiphenylamine sulfate hydrate and aniline/*N*-phenyl-1,4-phenylene diamine with APS as oxidant, followed by characterized by ¹H NMR, FTIR and MS spectroscopy. Subsequently, the organo-soluble EPI (EPI-3 and EPI-4) was prepared by reacting AT3/AT4 with dianhydride to give electroactive poly(amic acid) (EPAA), followed by reaction with suitable amount of pyridine to convert EPAA into EPI (*i.e.*, chemical imidization). The as-prepared organo-soluble EPI was characterized by FTIR and GPC spectroscopy. The solubility of as-prepared EPI was studied in six common organic solvents. Moreover, organo-soluble EPI-4 powder was immersed in 19 mL of 0.10 mM HAuCl₄ solution for 6 h to give EPI doped with gold nanoparticles (GNPs) (or EPI-4G). The appearance of GNPs onto the surface of EPI was confirmed by XRD, SEM-EDS and TEM. The redox capability of as-prepared materials was found to show the decreasing trend of EPI-4G > EPI-4 > EPI-3 based on the electrochemical CV studies. The as-prepared carbon paste electrode (CPE) modified with EPI-4G was found to reveal higher sensitivity, a relatively low LOD and a broad LDR in AA detection as compared to that of CPE modified with EPI-4, EPI-3 and bare CPE based on the CV responses. Moreover, the CPE modified with EPI-4G was found to exhibit excellent selectivity for the tertiary mixtures of AA/DA/UA, and three distinct voltammetric peaks can be resolved at three specific potentials as compared to those of other electrodes.

Acknowledgements

The author acknowledges financial support from the Ministry of Science and Technology, Taiwan, R.O.C (MOST 104-2113-M-033-001-MY3 and MOST 104-2923-M-033-001-MY2) as well as the Department of Chemistry at Chung Yuan Christian University, and the Department of Science and Technology (through the Manila Economic and Cultural Office), and University of St. Thomas

References

- [1] L. Hu, L. Deng, S. Alsaiani, D. Zhang, N.M. Khashab, *Anal. Chem.* 86 (2014) 4989–4994.
- [2] H. Bi, A.C. Fernandes, S. Cardoso, P. Freitas, *Sens. Actuator B-Chem.* 224 (2016) 668–675.
- [3] C. Lou, W. Liu, X. Liu, J. Chromatogr. B 969 (2014) 29–34.
- [4] N. Xia, L. Liu, R. Wu, H. Liu, S.J. Li, Y. Hao, *J. Electroanal. Chem.* 731 (2014) 78–83.
- [5] G.P. Keeley, N. McEvoy, H. Nolan, M. Holzinger, S. Cosnier, *G.S. Chem. Mat.* 26 (2014) 1807–1812.
- [6] D. Micić, B. Šljukić, Z. Zujovic, J. Travas-Sejdic, G. Ćirić-Marjanović, *Electrochim. Acta* 120 (2014) 147–158.
- [7] S. Pakpongpan, J.P. Mensing, D. Phokharatkul, T. Lomas, A. *Electrochim. Acta* 133 (2014) 294–301.
- [8] U. Rana, N.D. Paul, S. Mondal, C. Chakraborty, S. Malik, Water soluble polyaniline coated electrode: a simple and nimble electrochemical approach for ascorbic acid detection, *Synth. Met.* 192 (2014) 43–49.
- [9] M.M. Sk, C.Y. Yue, *J. Mater. Chem. A* 2 (2014) 2830–2838.
- [10] C. Xue, X. Wang, W. Zhu, Q. Han, C. Zhu, J. Hong, X. Zhou, H. Jiang, *Sens. Actuator B-Chem.* 196 (2014) 57–63.
- [11] C. Zhou, Y. Shi, J. Luo, L. Zhang, D. Xiao, *J. Mater. Chem. B* 2 (2014) 4122–4129.
- [12] T. Wu, L.Y. Wang, S. Du, W.J. Guo, M.S. Pei, *RSC Adv.* 5 (2015) 69067–69074.
- [13] K. Shanmugasundaram, G. Sai Anand, A.I. Gopalan, H.G. Lee, H.K. Yeo, S.W. Kang, K.P. Lee, *Sens. Actuator B-Chem.* 228 (2016) 737–747.
- [14] H. Zhao, H. Yin, Y. Yang, *RSC Adv.* 6 (2016) 29624–29628.
- [15] Y. Wei, C.C. Yang, T.Z. Ding, *Tetrahedron Lett.* 37 (1996) 731–734.
- [16] L. Chen, Y. Yu, H.P. Mao, X.F. Lu, W.J. Zhang, Y. Wei, *Mater. Lett.* 59 (2005) 2446–2450.
- [17] K.Y. Huang, C.L. Shiu, P.S. Wu, Y. Wei, J.M. Yeh, W.T. Li, *Electrochim. Acta* 54 (2009) 5400–5407.
- [18] C.J. Weng, J.Y. Huang, K.Y. Huang, Y.S. Jhuo, M.H. Tsai, J.M. Yeh, *Electrochim. Acta* 55 (2010) 8430–8438.
- [19] T.C. Huang, T.C. Yeh, H.Y. Huang, W.F. Ji, C.A. Chen, T.C. Lin, J.M. Yeh, *Electrochim. Acta* 63 (2012) 185–191.
- [20] C.W. Peng, C.H. Hsu, K.H. Lin, P.L. Li, Y. Wei, J.M. Yeh, Y.H. Yu, *Electrochim. Acta* 58 (2011) 614–620.
- [21] L.C. Yeh, T.C. Huang, Y.P. Huang, H.Y. Huang, H.H. Chen, T.I. Yang, J.M. Yeh, *Electrochim. Acta* 94 (2013) 300–306.
- [22] K.C. Chang, K.Y. Huang, M.C. Lai, W.I. Hung, S.C. Hsu, Y.K. Tsai, C.J. Weng, Y.S. Jhuo, J.M. Yeh, *Eur. Polym. J.* 56C (2014) 26–32.
- [23] Y. Xiao, F. Patolsky, E. Katz, J.F. Hainfeld, I. Willner, 199 (2003) 1877–1881.
- [24] M. Schierhorn, S.J. Lee, S.W. Boettcher, G.D. Stucky, M. Moskovits, *Adv. Mater.* 18 (2006) 2829–2832.
- [25] H. Cai, Y. Xu, N. Zhu, P. He, Y. Fang, *Analyst* 127 (2002) 803–808.
- [26] J. Wang, R. Polsky, D. Xu, *Langmuir* 17 (2001) 5739–5741.
- [27] J. Wang, D. Xu, R. Polsky, *J. Am. Chem. Soc.* 124 (2002) 4208–4209.
- [28] K.Y. Huang, C.L. Shiu, P.S. Wu, Y. Wei, J.M. Yeh, W.T. Li, *Electrochim. Acta* 54 (2009) 5400–5407.
- [29] L. Gu, S. Liu, H. Zhao, H. Yu, *RSC Adv.* 5 (2015) 56011–56019.
- [30] C.J. Weng, K.Y. Huang, Y.S. Jhuo, Y.L. Chen, C.F. Feng, C.M. Chien, J.M. Yeh, *Polym. Int.* 61 (2012) 205–212.
- [31] I. Róalska, P. Kutyk, I. Kulszewicz-Bajer, *New J. Chem.* 28 (2004) 1235–1243.
- [32] K.C. Chang, H.I. Lu, C.W. Peng, M.C. Lai, S.C. Hsu, M.H. Hsu, Y.K. Tsai, C.H. Chang, W.I. Hung, Y. Wei, J.M. Yeh, *ACS Appl. Mater. Interfaces* 5 (2013) 1460–1467.
- [33] S.C. Hsu, H.T. Cheng, P.X. Wu, C.J. Weng, K.S. Santiago, J.M. Yeh, *Electrochim. Acta* 238 (2017) 246–256.
- [34] A.J. Bard, L.R. Faulkner, Wiley, New York, 2001.
- [35] W. Shi, C. Liu, Y. Song, N. Lin, S. Zhou, X. Cai, *Biosens. Bioelectron.* 38 (2012) 100–106.
- [36] T.C. Huang, T.C. Yeh, H.Y. Huang, W.F. Ji, Y.C. Chou, W.I. Hung, J.M. Yeh, M.H. Tsai, *Electrochim. Acta* 56 (2011) 10151–10158.
- [37] L.C. Yeh, T.C. Huang, F.Y. Lai, G.H. Lai, A.Y. Lo, S.C. Hsu, T.I. Yang, J.M. Yeh, *Surf. Coat. Technol.* 303 (2016) 154–161.
- [38] T.C. Huang, L.C. Yeh, H.Y. Huang, Z.Y. Nian, Y.C. Yeh, Y.C. Chou, J.M. Yeh, M.H. Tsai, *Polym. Chem.* 5 (2014) 630–637.
- [39] A. Ambrosi, A. Morrin, M.R. Smyth, A.J. Killard, The application of conducting polymer nanoparticle electrodes to the sensing of ascorbic acid, *Anal. Chim. Acta* 609 (2008) 37–43.
- [40] W. Kit-Anan, A. Olarnwanich, C. Sriprachubwong, C. Karuwan, A. Tuantranont, A. Wisitsoraat, W. Srituravanich, A. Pimpin, *J. Electroanal. Chem.* 685 (2012) 72–78.
- [41] J. Huang, Y. Liu, H. Hou, T. You, *Bioelectron* 24 (2008) 632–637.
- [42] F. Sekli-Belaidi, P. Temple-Boyer, P. Gros, *J. Electroanal. Chem.* 647 (2010) 159–168.
- [43] F. Sekli-Belaidi, P. Temple-Boyer, P. Gros, *J. Appl. Polym. Sci.* 134 (2017) 44351–44360.